SSCL-474

SSCL-474

Superconducting Super Collider

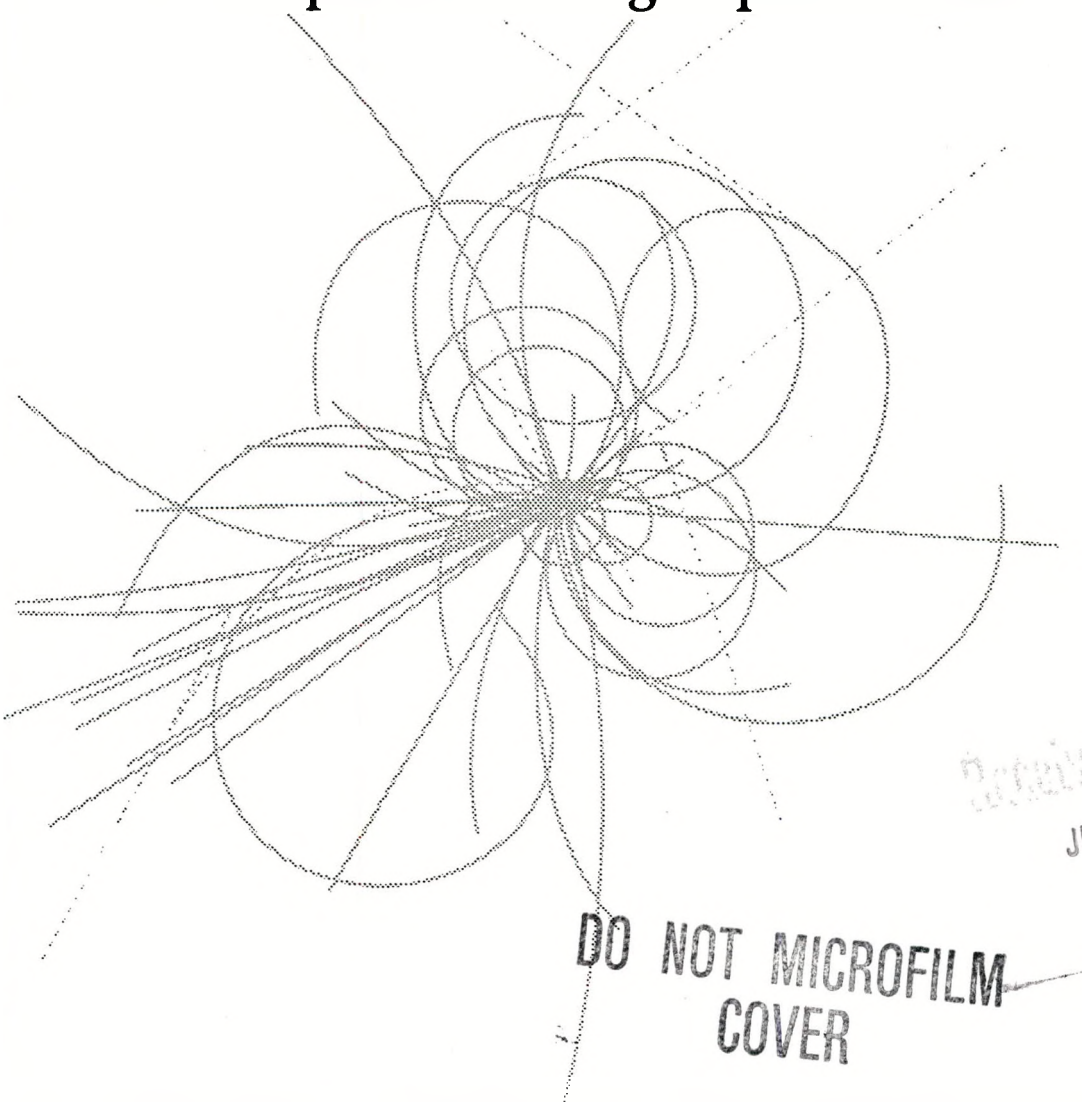

Cooldown and Warmup Computer Simulations of the SSC Ring

R. H. Carcagno, W. E. Schiesser, and A. Yücel

June 1991

To be published in Advances in Cryogenic Engineering 37, Plenum Press, New York

SSCL--474

DE91 015278

Cooldown and Warmup Computer Simulations of the SSC Ring*

R. H. Carcargno, W. E. Schiesser, and A. Yücel

Accelerator Division
Superconducting Super Collider Laboratory†
2550 Beckleymeade Ave.
Dallas, TX 75237

June 1991

---

*Presented at the 1991 Cryogenic Engineering Conference, University of Alabama-Huntsville, June 10-14, 1991.

†Operated by the Universities Research Association, Inc., for the U.S. Department of Energy under Contract No. DE-AC02-89ER40486.

COOLDOWN AND WARMUP COMPUTER SIMULATIONS OF THE SSC RING

R. H. Carcagno, W. E. Schiesser and A. Yücel

Cryogenics Group, Accelerator Division
Superconducting Super Collider Laboratory*
Dallas, Texas

ABSTRACT

The Superconducting Super Collider (SSC) consists of two stacked rings of superconducting magnets; each ring is about 86 km in circumference. The total mass to be cooled to liquid helium temperature amounts to about 1×10^8 kg, and the total helium inventory under nominal operating conditions (4.15 K and 4 atm) is about 2.8×10^5 kg. The cooldown and warmup process of a long string of magnets has to be well understood in order to design a cryogenic system that can satisfy the requirements of helium inventory handling, magnet temperature gradients, and process time for the different cooldown and warmup scenarios being planned for the SSC. A system that can be convincingly simulated can be understood, controlled, operated and improved in a systematic way.

In this paper, we introduce two numerical models, a lumped model and a distributed model, for cooldown and warmup of the SSC ring, and present simulation results for an SSC string (4320 m long, or 1/20th of the full ring circumference). The models cover the temperature range between room and liquid helium temperature; the distributed model includes radial temperature distribution in the cold mass. Low temperature range simulations are particularly important to study inventory handling strategies because of the relationship between rapid changes in density and the system mass flow rate.

INTRODUCTION

The SSC will contain some 10,000 superconducting magnets of many types in the two collider rings. An extensive cryogenic system is needed to maintain these magnets at or below the operating temperature of 4.35 K under various operating conditions[1]. Multiple refrigeration units that are capable of independent operation, but interconnected for redundancy, were selected to facilitate parallel construction and operation. Thus the rings are subdivided into ten cryogenic sectors. Each ring sector has two strings: one upstream and one downstream from the local refrigerator. The basic unit of a string is the half-cell which

*Operated by the Universities Research Association, Inc., for the U.S. Department of Energy under Contract No. DE-AC02-89ER40486.

consists of five dipole magnets, a quadrupole magnet and a spool piece. Two such half-cells constitute one cell which is 180 m long. Six cells form a section, and four sections make up the string. The magnets are cooled by single phase helium flow which passes through the magnets in series. This stream is recooled at the end of each cell, i.e., 24 times along the string. At the sector boundary, the flow is returned to the refrigeration plant through a pipe running parallel to the magnet string inside the cryostat.

A wide variety of steady and transient system operating conditions can be identified in the yearly cycle of operation of the collider. Initial cooldown of the magnet strings, and warmup and subsequent cooldown of sections for magnet maintenance are two of the transient operating conditions that must be provided for in the refrigeration system design. Simulations of cooldown and warmup of the magnet system are essential for understanding, control and improvement of the system performance. This study presents two computer models and simulation results for cooldown and warmup of SSC magnets by helium flow through the cooling channels. Unlike previous studies[2-4], the present models account for temperature and pressure dependence of material properties, and extend the simulations to very low temperatures.

ANALYSIS

Figure 1 shows a cross section of the SSC dipole magnet, including the iron yoke and the four cooling channels. Helium flowing through the cooling channels exchanges heat with the iron yoke. During cooldown and warmup, the heat leak into the iron yoke from the outside is negligible compared to the heat transfer between the the iron and helium.

Helium Equations:

We consider one-dimensional flow of helium in the cooling channels, and neglect axial conduction and kinetic energy effects. The governing equations are:

Helium mass conservation:

$$A\frac{\partial \rho_g}{\partial t} + \frac{\partial w_g}{\partial x} = 0 \qquad (1)$$

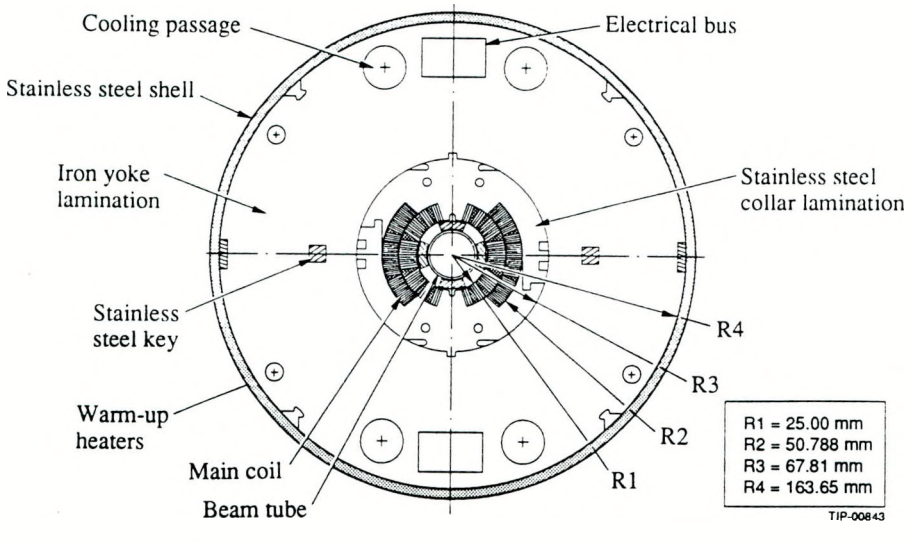

Figure 1. Cross section of the SSC Dipole magnet.

Helium energy:

$$\rho_g \frac{Dh_g}{Dt} \equiv \rho_g \frac{\partial h_g}{\partial t} + \frac{w_g \partial h_g}{A \partial x} = \frac{Dp}{Dt} + hP(T_i - T_g) \tag{2}$$

Letting $dh_g = C_{pg}\, dT_g$, we have

$$\tau_g \frac{\partial T_g}{\partial t} + \lambda_g \frac{\partial T_g}{\partial x} = \frac{A}{hP} \frac{Dp}{Dt} + T_i - T_g \tag{3}$$

The characteristic time τ_g and the characteristic length λ_g in Eq. (2b) are given by

$$\tau_g = \frac{C_{pg}\, A\, \rho_g}{h\, P} \qquad \text{and} \qquad \lambda_g = \frac{C_{pg}\, w_g}{h\, P}$$

Helium pressure:

$$-\frac{\partial p}{\partial x} = 2 \frac{f}{D} \left(\frac{w_g}{A}\right)^2 \frac{1}{\rho_g} \tag{4}$$

The friction factor f is based on the nominal flow conditions and the corresponding nominal pressure drop specified in the Site-Specific Design Report[5]. The heat transfer coefficient h is given by the single-phase turbulent flow correlation:

$$h = 0.023 \frac{w_g}{A} C_{pg}\, Re^{-0.2}\, Pr^{-2/3} \left(\frac{\mu_g}{\mu_i}\right)^{0.14} \tag{5}$$

Iron Temperature:

We consider two separate models to compute the iron temperature:

a) Lumped model: The iron yoke accounts for about 3/4 of the total cold mass. We assume that all the dipole mass is composed of iron and neglect transverse conduction in the iron in this model. Axial conduction in the cold mass is also neglected since the stainless steel collars and the iron yoke are composed of laminations. Under these assumptions, the iron temperature is governed by

$$\tau_i \frac{\partial T_i}{\partial t} = T_g - T_i \tag{6}$$

The characteristic length τ_i for the iron is given by:

$$\tau_i = \frac{C_{pi}\, m'_i}{h\, P}$$

b) Distributed model: This model considers the radial temperature distributions in the coils, collars and yoke (Figure 2). Azimuthal (θ) variations are neglected. The governing equations for the coil and collar temperatures are:

$$\rho_j C_{pj} \frac{\partial T_j}{\partial t} = \frac{1}{r} \frac{\partial}{\partial r} \left(r\, k_j \frac{\partial T_j}{\partial r}\right) \qquad j = 1,2 \tag{7}$$

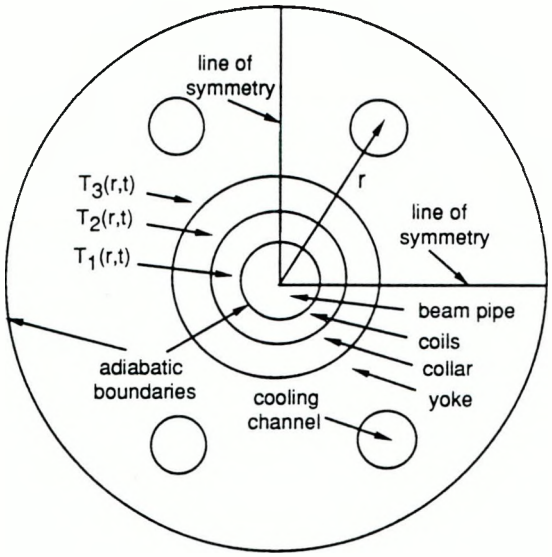

Figure 2. Distributed model for the SSC dipole magnet.

Axial conduction in the coils was allowed but found to be negligible. The helium channel in the yoke is treated as a point source. The temperature distribution in the iron yoke is given by:

$$\rho_3 C_{p3} \frac{\partial T_3}{\partial t} = \frac{1}{r} \frac{\partial}{\partial r}\left(r\, k_3 \frac{\partial T_3}{\partial r}\right) + q''' \tag{8}$$

where q''' is the volumetric heat source (or sink) at $r = r_c$ and represents the heat exchange between the yoke and helium along the cooling channel surface.

The iron temperature T_i in Eq. (3) is given by T_3 at $r = r_c$ in this model.

The boundary conditions are:

$$k_1 \frac{\partial T_1}{\partial r} = 0 \qquad \text{at} \quad r = r_0 \tag{9}$$

$$k_j \frac{\partial T_j}{\partial r} = c_{12}(T_2 - T_1) \qquad \text{at} \quad r = r_1, \quad j = 1,2. \tag{10}$$

$$k_j \frac{\partial T_j}{\partial r} = c_{23}(T_3 - T_2) \qquad \text{at} \quad r = r_2, \quad j = 2,3. \tag{11}$$

$$k_3 \frac{\partial T_3}{\partial r} = 0 \qquad \text{at} \quad r = r_3 \tag{12}$$

where c_{12} and c_{23} represent contact conductance (inverse resistance) between the coils and collars, and between the collars and the yoke, respectively. The contact conductance at the coil-collar interface is taken as the thermal conductance of kapton insulation between the coils and collars. The contact resistance at the collar-yoke interface is negligible as the yoke and collars are in good thermal contact.

Material Properties. We consider material property dependence on temperature for the cold mass and helium, as well as on pressure for the latter. The properties for the iron yoke,

stainless steel collars and the coils are computed using NBS compilations[6]. The helium properties are also obtained from NBS tabulations[7].

Solution Method. We use an explicit finite difference scheme to solve Eqs. (1-6). Upwind differencing for the advection terms is employed in this scheme. Spatial and time steps are selected to be small compared to the iron and helium characteristic lengths and times for stability and accuracy. Details of the discretization of the governing equations are given by Carcagno[8].

The distributed model is a mixed system of parabolic-hyperbolic partial differential equations (PDEs) - parabolic for the radial conduction of heat in the cold mass and hyperbolic for the flow of helium through the magnets. This mixed system was integrated by the numerical method of lines[9] with the time integration performed by a sparse matrix, BDF (Gear) integrator, subroutine LSODES. Three point, second order finite differences were used to approximate the spatial derivatives in the cold mass PDEs, and two point upwind finite differences were used to approximate the spatial derivatives in the helium PDEs. Stability and accuracy in the calculations was achieved by the implicit, variable step, variable order features of LSODES. Convergence in the approximation of spatial derivatives was tested by varying the number of grid points.

COOLDOWN RESULTS

In this section we present simulation results for the 300 K to 80 K phase of the cooldown of the magnet system specified in the Site-Specific Conceptual Design Report. The basic unit for cooldown operations is a string which consists of 24 cells. Since cooling proceeds as a wave, the room temperature gas is removed from the string through cooldown valves located at every cell. Therefore the 300 K helium gas flows through one cell only, while the 80 K helium passes through the whole string.

The magnet length selected for these simulations is 180 m (one cell length). A quasi-steady temperature profile front rapidly develops over this length. The results can be extrapolated to the entire string since the cold front travels at approximately.constant speed. The simulation parameters are listed below:

Channel diameter = 0.03175 m
Helium pressure at entrance = 10 atm (10^6Pa)
Helium mass flow rate at entrance = 0.1 kg/s (0.025 kg/s per channel)

In the lumped model, cold mass per unit length is taken as 652 kg/m (163 kg/m per channel). Figure 3 shows the helium and iron temperature profiles along the cell length at 4-hr intervals. Cooldown of the cell takes approximately 24 hours, with the cold front advancing at 8.40 m/hr. Extrapolating to the entire string (4320 m), cooldown would require about 22 days.

The maximum longitudinal (axial) temperature gradient for the quasi-steady iron temperature profile is 8.5 K/m. However, with the step change in helium temperature at the entrance from 300 K to 80 K, the cold mass near the entrance is initially subjected to considerably higher temperature gradients. Instead of a step change, the cold gas temperature at the entrance can be lowered or ramped down from 300 K to 80 K gradually in order to control the temperature gradients and the associated mechanical stresses in the magnets at the beginning. A linear ramp of 4 hours was found to be sufficient to limit the initial values of temperature gradients to the above asymptotic value (8.5 K/m).

Cooldown predictions by the distributed model are presented in Figures 4-6. These results were obtained by using 20 grid points across the cold mass and 361 grid points along

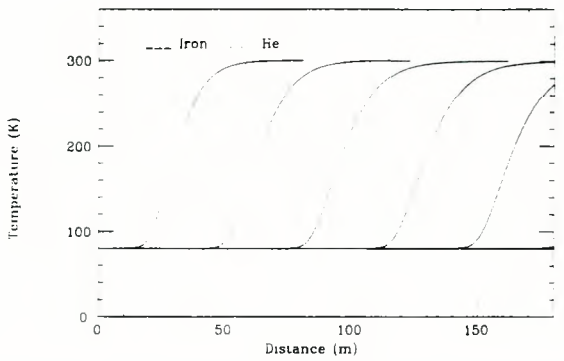

Figure 3. Helium and iron temperature profiles along an SSC cell at 4 hour intervals during cooldown from 300 K to 80 K (lumped model).

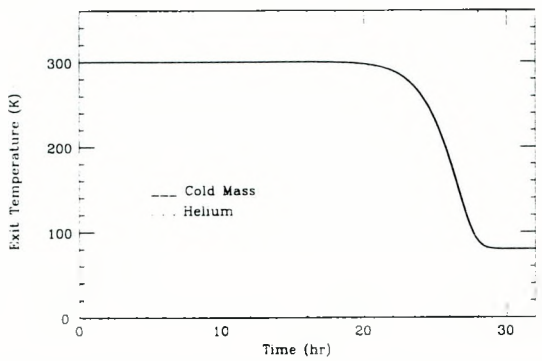

Figure 4. Coil, collar and yoke midpoint temperatures and helium temperature at the exit of an SSC cell during cooldown from 300 K to 80 K.

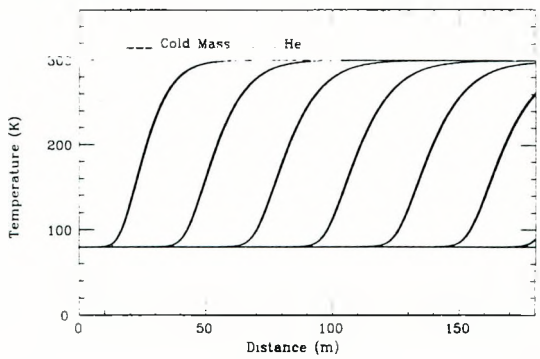

Figure 5. Helium and iron temperature profiles along an SSC cell at 4 hour intervals during cooldown from 300 K to 80 K (distributed model).

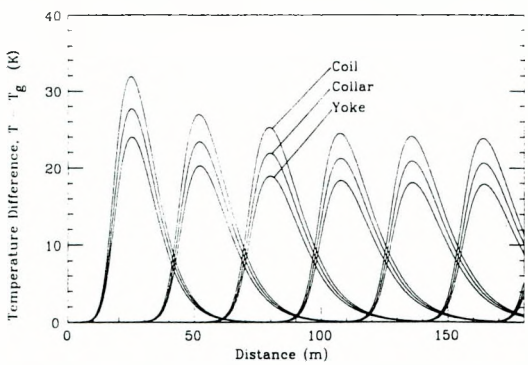

Figure 6. Differences between the coil, collar and yoke midpoint temperatures and helium temperature along an SSC cell at 4 hour intervals during cooldown from 300 K to 80 K.

one cell of magnets resulting in a total of 7220 ordinary differential equations in time. As expected, it takes longer to cool the magnets when radial diffusion of heat in the cold mass is taken into account (Figure 4). The cold front advances at a rate of 8.05 m/hr: total cooldown time is about 5% more than that predicted by the lumped model. The decrease in the cooldown speed is accompanied by a decrease in the asymptotic maximum temperature gradient to 8.10 K/m (Figure 5). Given the scales of Figures 4 and 5, it is difficult to distinguish the coil, collar and yoke temperatures. Figure 6 presents the coil, collar and yoke midpoint temperatures relative to the local helium temperature. The development of the quasi-steady temperature profiles over the length of the cell is evident from the figure.

WARMUP RESULTS

We present in this section simulation results for warmup of a string (4320 m) from 4.15 K to 20 K. The inlet pressure is 10 atm (10^6Pa) and the inlet mass flow rate is 0.050 kg/s (0.0125 kg/s per channel). For these calculations, the lumped model included a detailed structure of the string (the dipoles, quadrupoles, spool pieces and the interconnect regions). The effect of helium contained between the laminations in the magnets was also considered.

Temperature distributions along the string are shown in Figure 7. During warmup, the situation is different than cooldown. There is no distinct hot front advancing at constant velocity. Instead, we observe temperature profiles advancing at temperature-dependent velocities which decrease with increasing temperature. Thus the temperature profiles tend to extend over the length of the string. In the initial stages of warmup, when the warm gas arrives at a given point along the string, the iron temperature at this point rises rapidly to about 7-8 K. It takes relatively short time (about 3 hours) for the end of the string to reach this level. The reason for this is the low specific heat of iron around 4 K. A small change in the helium enthalpy is sufficient to increase the iron temperature a few Kelvin from liquid helium temperatures. As the iron temperature rises, however, its specific heat increases sharply (from 0.38 J/kg-K at 4 K to 1.24 J/kg-K at 10 K, for example). As a result, increasingly more helium energy has to be spent to raise the iron temperature. Warmup thus proceeds at a slower pace after the above initial stage. This is evidenced by the decreasing rate of change of the iron temperature at the end of the string (Figure 8). Warmup of the string to 20 K is completed in about 14 hours.

The helium mass flow rate at the end of the string is shown in Figure 9. During the first 3 hours of warmup, the exiting mass flow rate is about 5 times the input mass flow rate. This is brought about by large changes in the local helium density as the small front of a few K moves rapidly through the string. Following the arrival of this mini front, helium mass flow rate at the exit drops gradually to its nominal value. The total amount of helium spent to warm the string to 20 K is about 2500 kg.

The oscillations observed in the exit mass flow rate are the result of the explicit scheme used in the calculations. The calculations could not be carried out for more than one hour of simulation time with the Dp/Dt term in the helium energy equation as the numerical scheme became unstable. This term was subsequently dropped in carrying out the full length simulations, but its magnitude was checked and verified to be negligible compared to the other terms in the energy equation. It was also necessary to ramp the temperature of the inlet gas to 20 K over a short period (300 seconds) for stability.

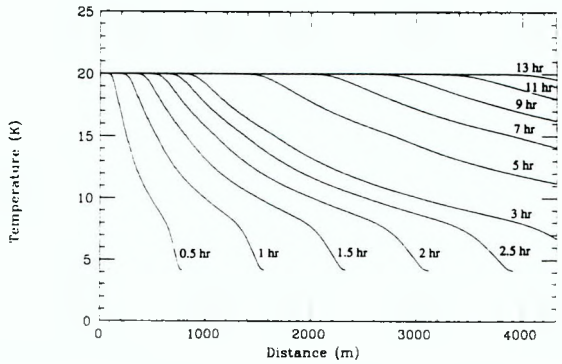

Figure 7. Iron temperature profiles along an SSC string during warmup from 4.15 K to 20 K (lumped model).

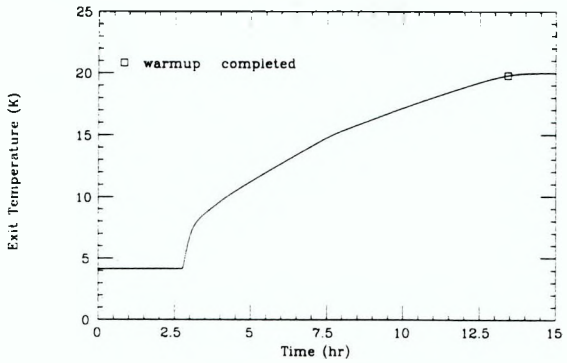

Figure 8. Helium temperature at the exit of an SSC string during warmup from 4.15 K to 20 K.

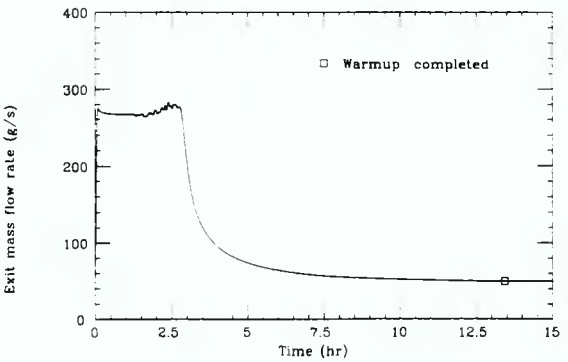

Figure 9. Helium mass flow rate at the exit of an SSC string during warmup from 4.15 K to 20 K.

CONCLUDING REMARKS

A lumped model for simulation of cooldown and warmup of SSC magnets is presented. The model allows full variation of material properties and extends the simulations to very low temperatures. A second distributed model which allows radial temperature distributions across the magnets is also presented. Results for cooldown of magnets from 300 K to 80 K, and for warmup of a string from 4.15 K to 20 K are discussed. The present models are capable of analyzing a variety of cooldown and warmup scenarios. The lumped model has been used to study the feasibility of employing intermediate temperature levels during cooldown, and the effects of varying the inlet gas temperature and mass flow rate on cooldown of magnets.

NOMENCLATURE

A	Cross-sectional area of cooling channel
c_{12}, c_{23}	Contact conductance
C_p	Specific heat
D	Diameter of cooling channel
f	Friction factor
h	Heat transfer coefficient
h_g	Helium enthalpy
k	Thermal conductivity
m_i'	Iron mass per unit length
P	Perimeter of cooling channel
p	Helium pressure
Pr	Prandtl number, $\mu C_p/k$
r	Radial distance
Re	Reynolds number, $w_g D/A\mu$
T	Temperature
t	time
w_g	Helium mass flow rate
x	Axial distance
λ	Characteristic length
μ	Viscosity
ρ	Density
τ	Characteristic time

Subscripts

g	Helium
i	Iron in the lumped model
1	Coils in the distributed model
2	Collars in the distributed model
3	Yoke in the distributed model

REFERENCES

1. M. S. McAshan and D. S. Finan, "Cryogenic System for the Superconducting Super Collider (SSC)," ASME Winter Annual Meeting, Dallas, TX (November 1990).

2. D. P. Brown and K. C. Wu, "Cooldown Calculations for SSC Magnets," SSC-N-21 (November 1984).

3. R. P. Shutt, "Cooldown of SSC Magnets," SSC-N-133 (March 1986).

4. G. Horlitz et al, Computer calculations on steady-state operation and different modes of cool down and warm up of the HERA superconducting proton ring, in: *Advances in Cryogenic Engineering*, Vol. 31, Plenum Press, New York (1986), p. 723.

5. "Site-Specific Conceptual Design of the Superconducting Super Collider," SSCL-SR-1056 (July 1990).

6. "Properties of Materials at Low Temperatures (Phase 1), a Compendium," U. J. Johnson, ed., Pergamon Press, New York (1961).

7. V. D. Arp and R. D. McCarty, "Thermophysical Properties of Helium-4 from 0.8 to 1500 K with Pressures to 2000 MPa," NIST Technical Note 1334 (1989).

8. R. C. Carcagno, "A Cooldown/Warmup Computer Model for the SSC," SSC-N-385 (September 1987).

9. W. E. Schiesser, "The Numerical Method of Lines Integration of Partial Differential Equations," Academic Press, San Diego (1991).